Gretel Smith, Esq.
State Bar No. 272769
Staff Counsel
Helping Hand Tools
P.O. Box 152994
San Diego, CA 92195
619-822-6261
Attorney for Rob Simpson and Helping Hand Tools

BEFORE THE ENERGY RESOURCES CONSERVATION AND DEVELOPMENT COMMISSION OF THE STATE OF CALIFORNIA

1516 NINTH STREET, SACRAMENTO, CA 95814

1-800-822-6228 – WWW.ENERGY.CA.GOV

APPLICATION FOR CERTIFICATION	**Docket No. 11-AFC-01**

Rob Simpson's and Helping Hand Tools Supplement Comments to the PMPD
Part 3 of 5

The following 11 emails and attachments were submitted to all parties on or about September 5, 2012. Mr. Simpson and Helping Hand Tools submits this document for public comment.

Respectfully submitted.

Date: September 11, 2012

/s/ Gretel Smith , Esq.

Gretel Smith, Esq.

Attorney for Helping Hand Tools &

Rob Simpson

Email 5 of 11

Email 5 of 11

From: <rob@redwoodrob.com>
Date: Wed, Sep 5, 2012 at 9:06 AM
Subject: Pio Pico PMPD comments Rob Simpson 5
To:
Cc: "Scott, Diane@Energy" <Diane.Scott@energy.ca.gov>, "djenkins@apexpowergroup.com" <djenkins@apexpowergroup.com>, "MFitzgerald@sierraresearch.com" <MFitzgerald@sierraresearch.com>, "jamckinsey@stoel.com" <jamckinsey@stoel.com>, "mafoster@stoel.com" <mafoster@stoel.com>, "e-recipient@caiso.com" <e-recipient@caiso.com>, "rob@redwoodrob.com" <rob@redwoodrob.com>, "Gretel.smith79@gmail.com" <Gretel.smith79@gmail.com>, "swilliams@scmv.com" <swilliams@scmv.com>, "Peterman, Carla@Energy" <Carla.Peterman@energy.ca.gov>, "Douglas, Karen@Energy" <Karen.Douglas@energy.ca.gov>, "Renaud, Raoul@Energy" <Raoul.Renaud@energy.ca.gov>, "Bartridge, Jim@Energy" <Jim.Bartridge@energy.ca.gov>, "Lemei, Galen@Energy" <Galen.Lemei@energy.ca.gov>, "Nelson, Jennifer@Energy" <Jennifer.Nelson@energy.ca.gov>, "Solorio, Eric@Energy" <Eric.Solorio@energy.ca.gov>, "kevinw.bell@energy.ca.gov" <kevinw.bell@energy.ca.gov>, "Allen, Eileen@Energy" <Eileen.Allen@energy.ca.gov>, Energy - Public Adviser's Office <PublicAdviser@energy.ca.gov>

Docket Number 11-AFC-01

Rob Simpson
Director
Helping Hand Tools (2HT)
1901 First Avenue, Ste. 219
San Diego, CA 92101
Rob@redwoodrob.com

-------- Original Message --------
Subject: Pio Pico PSD comments 2
From: <rob@redwoodrob.com>
Date: Wed, July 18, 2012 1:19 am
To: Kohn.Roger@epa.gov

Attached please find my initial Pio Pico PSD comments Pio Pico PSD comments

Rob Simpson
Executive Director
Helping Hand Tools
27126 Grandview Avenue
Hayward CA. 94542
Rob@redwoodrob.com

-------- Original Message --------
Subject: Pio Pico
From: <rob@redwoodrob.com>
Date: Wed, January 18, 2012 9:04 pm
To: "Steve Moore" <Steve.Moore@sdcounty.ca.gov>
Cc: "Staff April" <2htlegal@gmail.com>

Mr. Moore,

I will be sending a series of emails which constitute my comments for the Pio Pico PDOC. These attachments relate the Jacobson Effect and to localized effects of CO2 and other pollutants

Thank you

Rob Simpson

jacobson link.pdf
222K View Download
jacobson effect.pdf
493K View Download

Attachment 1 of 2 to
Email 5 of 11

GEOPHYSICAL RESEARCH LETTERS, VOL. 35, L03809, doi:10.1029/2007GL031101, 2008

On the causal link between carbon dioxide and air pollution mortality

Mark Z. Jacobson[1]

Received 22 June 2007; revised 14 December 2007; accepted 3 January 2007; published 12 February 2008.

[1] Greenhouse gases and particle soot have been linked to enhanced sea-level, snowmelt, disease, heat stress, severe weather, and ocean acidification, but the effect of carbon dioxide (CO_2) on air pollution mortality has not been examined or quantified. Here, it is shown that increased water vapor and temperatures from higher CO_2 separately increase ozone more with higher ozone; thus, global warming may exacerbate ozone the most in already-polluted areas. A high-resolution global-regional model then found that CO_2 may increase U.S. annual air pollution deaths by about 1000 (350–1800) and cancers by 20–30 per 1 K rise in CO_2-induced temperature. About 40% of the additional deaths may be due to ozone and the rest, to particles, which increase due to CO_2-enhanced stability, humidity, and biogenic particle mass. An extrapolation by population could render 21,600 (7400–39,000) excess CO_2-caused annual pollution deaths worldwide, more than those from CO_2-enhanced storminess. Citation: Jacobson, M. Z. (2008), On the causal link between carbon dioxide and air pollution mortality, Geophys. Res. Lett., 35, L03809, doi:10.1029/2007GL031101.

1. Introduction

[2] Because carbon dioxide's (CO_2's) ambient mixing ratios are too low to affect human respiration directly, CO_2 has not been considered a classic air pollutant. Its effects on temperatures, though, affect meteorology, and both feed back to air pollution. Several studies have modeled the sensitivity of ozone to temperature [Sillman and Samson, 1995; Zhang et al., 1998] and the regional or global effects of climate change from all greenhouse gases on ozone [Thompson et al., 1989; Evans et al., 1998; Dvortsov and Solomon, 2001; Mickley et al., 2004; Stevenson et al., 2005; Brasseur et al., 2006; Murazaki and Hess, 2006; Steiner et al., 2006; Racherla and Adams, 2006] and aerosol particles [Aw and Kleeman, 2003; Liao et al., 2006; Unger et al., 2006]. Some studies have highlighted the effect of water vapor on chemistry [Evans et al., 1998; Dvortsov and Solomon, 2001; Stevenson et al., 2005; Steiner et al., 2006; Racherla and Adams, 2006; Aw and Kleeman, 2003]. However, none has isolated the effect of CO_2 alone on ozone, particles, or carcinogens, applied population and health data to the pollution changes, or examined the problem with a global-regional climate/air pollution model.

[3] Here, a box photochemistry calculation is first used to show how increases in water vapor and temperature independently increase ozone more with high than low ozone. This analysis helps to explain the causal link between CO_2 and health in areas where most people live, as subsequently found in 3-D global-regional simulations.

2. Chemical Effects of CO_2 on Ozone

[4] The SMVGEAR II chemical solver was used first in box mode, without dilution or entrainment, to solve chemistry for 12 hours among 128 gases and 395 inorganic, organic, sulfur, chlorine, and bromine reactions (including 57 photoprocesses) (mostly given by Jacobson et al. [2007], also see the supplementary material of Jacobson [2007]). Cases with different initial NO_x and organic gas were run.

[5] Figure 1 shows the water-vapor (H_2O) and temperature-dependence of ozone under several ozone precursor combinations. For initial $NO_x < 8$ ppbv, ozone decreased with increasing H_2O. For initial $NO_x > 80$ ppbv and moderate initial NO_x with low organics, though, ozone increased with increasing H_2O, by up to 2.8 ppbv-O_3 per 1 ppthv-H_2O. Between these extremes, ozone increased with increasing H_2O at low H_2O and stayed constant or slightly decreased at high H_2O (see the auxiliary material).[1] Figure 1 also shows that, generally (but not always), increasing water vapor increased ozone more with higher ozone.

[6] Further, the more ozone present, the more temperature-dependent chemistry increases ozone (Figure 1), consistent with Sillman and Samson [1995] and Zhang et al. [1998]. The ozone increase (Dc, ppbv) per 1 K change in temperature (DT) from all points in Figure 1 were fit to

$$Dc/DT = -0.13034 - 0.0045585c + 0.00028643c^2 - 4.6893 \times 10^{-7}c^3 \quad (1)$$

where c is ozone (ppbv) at 298.15 K (32–250 ppbv). A 1 K rise increased ozone by about 0.1 ppbv at 40 ppbv but 6.7 ppbv at 200 ppbv. Olszyna et al. [1997] reported an observed correlation in the rural southeast U.S. of 2.4 ppbv ozone per 1 K. If temperature-dependent chemistry alone were causing this increase, ozone would need to be about 115 ppbv (equation 1) in that study, but it was 30–90 ppbv. Thus, other factors not accounted for in Equation 1, such as H_2O increases (described above) and biogenic gas emission increases [e.g., Guenther et al., 1995], due to higher temperatures, may have caused the larger observed temperature-ozone correlation. Also, both temperature and ozone increase with sunlight, so all observed temperature-ozone correlations overestimate the magnitude of cause and effect.

[1]Department of Civil and Environmental Engineering, Stanford University, Stanford, California, USA.

0094-8276/08/2007GL031101$05.00

[1]Auxiliary materials are available in the HTML. doi:10.1029/2007GL031101.

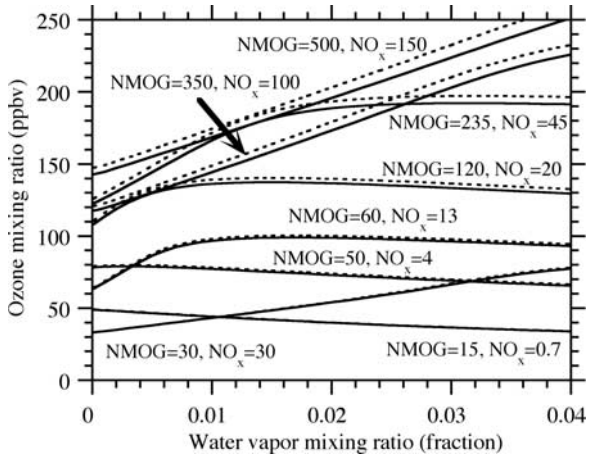

Figure 1. Mixing ratio of ozone and several other gases as a function of water vapor mixing ratio after 12 hours of a box-model chemistry-only simulation initialized at 0430 under several initial NO_x and nonmethane organic gas (NMOG) mixing ratio combinations (ppbv) (given in the figure) at 298.15 K (solid lines) and 299.15 K (dashed lines). The simulations assumed sinusoidally varying photolysis between 0600 and 1800.

3. Health Effects of CO_2 From Global-U.S. Simulations

[7] The chemistry used for Figure 1 was applied with emission, aerosol, cloud, meteorological, radiative, transport, and surface processes in the nested global-urban 3-D model, GATOR-GCMOM. The model (see auxiliary material) has been evaluated against U.S. gas, aerosol, meteorological, and radiative data extensively [e.g., Jacobson, 2001; Jacobson et al., 2004, 2007; Colella et al., 2005].

[8] Two global simulations (4°-SN × 5°-WE) were run under present-day conditions. In the second, fossil-fuel CO_2 (fCO_2) ambient mixing ratios and emissions were set to preindustrial values. When U.S. temperatures were about 1 K higher in the present minus preindustrial-CO_2 global simulations, the U.S. regional domain (0.5°S-N × 0.75°W-E) in each global simulation was turned on and initialized with global-domain data (including ambient CO_2). Global and regional domains were run another four months. Emissions of fCO_2 were included in the present-day but not preindustrial-CO_2 global- and U.S.-domain simulations.

[9] Figures 2 and S3 show differences between the present-day and preindustrial-CO_2 simulations. Figure 2a compares modeled with radiosonde (1958–2006) vertical temperature differences. The population-weighted near-surface temperature increase over land was 1.07 K (Table S4), which increased population-weighted H_2O by 1.28 ppthv (Table S4) and U.S.-averaged H_2O by 1.1 ppthv (Figure 2b). The observed 1961–1995 U.S. water vapor increase and positive correlation between temperature and H_2O [Gaffen and Ross, 1999] support the modeled H_2O increase with increasing temperatures.

[10] Figure 2c indicates that fCO_2 increased ozone by 0.12 ppbv in the U.S., 5 ppbv in Los Angeles, 1–5 ppbv in the southeast, and up to 2 ppbv along the northeast coast. In Los Angeles, the 0.75 K temperature increase (Figure 2a) and 1.3 ppthv water vapor increase increased ozone through chemistry (Figure 1).

[11] In the southeast, 0.5–1 K temperature increases increased isoprene and monoterpenes (Figure S3a), reducing the relative humidity (Figure S3c) and cloud optical depth (Figure S3d), increasing ultraviolet radiation (Figure S3e), and enhancing ozone. The 0.5–2 ppbv/K ozone increase in Tennessee is just below the correlated estimate of 2.4 ppbv/K from Olszyna et al. [1997] as expected (section 2). Averaged over the U.S. domain, higher temperatures from fCO_2 increased biogenic soil NO_x, isoprene, monoterpene, and other organic carbon emissions by 6% (0.01 Tg/yr), 9% (0.47), 9.8% (0.15), and 8.9% (0.14), respectively. In the northeast, higher ozone due to higher temperatures was offset partly by higher cloud optical depth (Figure S3d) and lower ultraviolet radiation (Figure S3e), modestly increasing ozone.

[12] The population-weighted 8-hr ozone increase due to fCO_2 was +0.72 ppbv (Table 1), suggesting a greater increase over populated than less-populated areas. FCO_2 increased particles in populated areas (Tables 1 and S4) by warming the air more than the ground, increasing stability (as with radiosonde data-Figure 2a, ii), decreasing turbulence, shearing stress, and surface wind speed (Table S4 and Figure S3), reducing dispersion. Reduced dispersion and wind speed are consistent with Mickley et al. [2004] who correlated warmer temperatures with reduced cyclone activity. FCO_2 also increased isoprene and monoterpene emissions, thus secondary organic matter (SOM) (Table S4, Figures S3a and S3b); and increased relative humidity (Table S4) by increasing H_2O, swelling aerosol particles, increasing nitric acid and ammonia dissolution and the surface area for sulfuric acid and organic condensation. FCO_2 increased land precipitation, consistent in direction with observed trends [Intergovernmental Panel on Climate Change, 2001], increasing aerosol removal, but less than other processes increased aerosol concentrations.

[13] Health effect changes (Dy) due to ozone and $PM_{2.5}$ changes in each model cell were determined from [e.g., Ostro et al., 2006],

$$\mathrm{Dy} = (1 - \exp[-\mathrm{b}\,\mathrm{Dx}])\mathrm{y}_0\mathrm{P} \qquad (2)$$

where Dx is the simulation-averaged mixing ratio or concentration change in the cell, b is the fractional increase in risk per unit Dx, y_0 is the baseline health effect rate, and P is the cell population exposed to at least a minimum threshold. Table 1 and its footnote provide values of P, Dx, b, y_0, and thresholds. Changes were summed over all cells and adjusted from a four-month to an annual average (Table 1, footnote).

[14] With this method, mortality increases due to modeled ozone and $PM_{2.5}$ from fCO_2 were 415 (207–620)/yr and 640 (160–1280)/yr, respectively, per 1.07 K (Table 1) or a total of near 1000 (350–1800) per 1.00 K (a 1.1% increase relative to the baseline death rate - Table 1), with about 40% due to ozone. A simple extrapolation from U.S. to world population (301.5 to 6600 million) gives 21,600 (7400–39,000) deaths/yr worldwide per 1 K due to fCO_2 above the baseline air pollution death rate (2.2 million/yr). The ozone portion of this (8,500 deaths/yr) is conservative compared with 15,500 deaths/yr, calculated from West et al. [2006] (= 30,000 deaths/yr from 1 ppbv ozone multiplied by the 2006:2030 population ratio (66:92) and the ozone

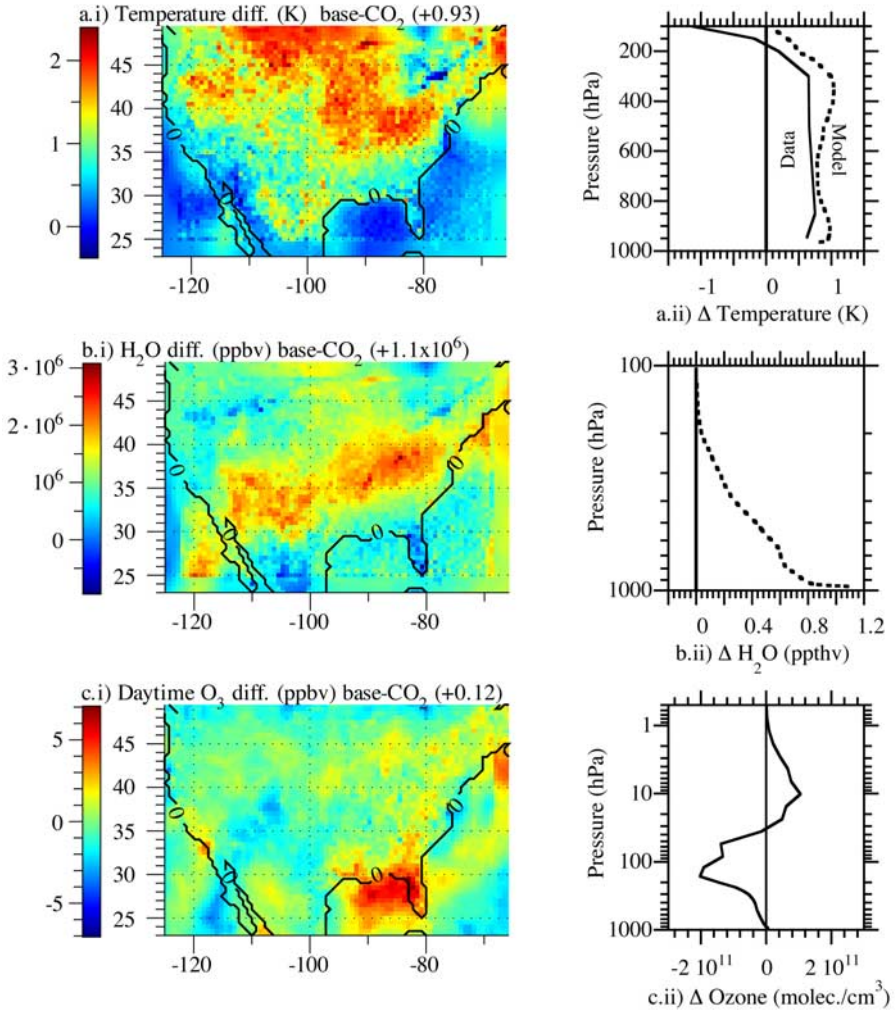

Figure 2. . Four-month (mid-July to mid-November) domain-averaged near-surface and vertical-profile differences in (a) temperature, (b) water vapor, and (c) ozone between the present-day and preindustrial-CO_2 simulations. The domain-averaged (over land and water) change for each surface plot is given in parentheses. Also shown in Figure 2a (ii) is the 1958–2006 globally-averaged radiosonde temperature change [Thorne et al., 2005], which is for reference only since the present simulations isolate the effects of CO_2 and do not examine all forcing agents.

change ratio (0.72:1.0). Remaining differences may be due to different thresholds used (35 ppbv here vs. 25 ppbv).

[15] One estimate of severe weather-related fatalities worldwide in the 1990s was 33,000/yr (Worldwatch Institute, Unnatural disaster: The lesson of Katrina, available at www.worldwatch.org/node/1822, 2005). A 1 K rise will increase this number, but less than 23,000/yr given that hurricane and tornado deaths have declined due to better warning systems (e.g., the deadliest hurricane since 1910 was over 30 years ago – Honduras, 1974, 10,000 deaths). Global warming will increase heat stress- and disease-related deaths as well, but by uncertain rates [e.g., Medina-Ramon and Schwartz, 2007].

[16] FCO_2 increased carcinogens, but the increase was small. Isoprene increases due to higher temperatures increased formaldehyde and acetaldehyde. Reduced dispersion increased exposure to these carcinogens and benzene and 1,3-butadiene.

[17] These simulations treated temperature effects on natural emissions but not power plant or vehicle emissions. A sensitivity test was run examining the impact of 1 K on power plant energy demand and emissions. The resulting ozone (Figure S4) may cause 80 more U.S. deaths/yr. However, warmer winter temperatures will also decrease natural gas and vehicle emissions, and warmer summers will increase vehicle emissions [Rubin et al., 2006; N. Motallebi et al., manuscript in review, 2007]. The feedbacks of temperature to anthropogenic emissions must be studied more but are expected to be smaller than the other feedbacks examined here. Further uncertainties arise from model resolution, current and future emissions, numerical treatments, health data, and extrapolation of four-month results to a year, as detailed in the auxiliary material.

4. Effects of CO_2 on Stratospheric Ozone and UV Radiation

[18] Whereas, fCO_2 warms the surface and troposphere, it cools the stratosphere (Figure 2a, ii). Measurements indicate a 1%/yr (0.45 ppmv/decade) stratospheric water vapor

Table 1. Summary of CO_2's Effects on Cancer, Ozone Mortality, Ozone Hospitalization, Ozone Emergency Room Visits, and Particulate-Matter Mortality[a]

	Base	Base Minus No fCO_2
	Carcinogens	
Formaldehyde (ppbv)	3.61	+0.22
Acetaldehyde (ppbv)	2.28	+0.203
1,3-Butadiene (ppbv)	0.254	+0.00823
Benzene (ppbv)	0.479	+0.0207
USEPA cancers/yr[b]	389	+23
OEHHA cancers/yr[b]	789	+33
	Ozone	
8-hr ozone (ppbv) in areas $\geq$35 ppbv[c]	42.3	+0.724
Pop (mil.) exposed in areas $\geq$35 ppbv[d]	184.8	184.8
High ozone deaths/yr[e]	6230	620
Med. ozone deaths/yr[e]	4160	+415
Low ozone deaths/yr[e]	2080	+207
Ozone hospitalizations/yr[e]	24,100	+2400
Ozone ER visits/yr[e]	21,500	+2160
	Particulate matter	
PM2.5 ($\mu g/m^3$) in areas > 0 $\mu g/m^3$[f]	16.1	+0.065
Pop (mil.) exposed in areas $\geq$ 0 $\mu g/m^3$	301.5	301.5
High PM2.5 deaths/yr[g]	191,000	+1280
Medium PM2.5 deaths/yr[g]	97,000	+640
Low PM2.5 deaths/yr[g]	24,500	+160

[a]Results are shown for the present-day ("Base") and present-day minus preindustrial ("no-fCO_2") 3-D simulations. All mixing ratios and concentrations are near-surface values averaged over four months (mid-July to mid-November) and weighted by population (population-weighted value is defined in the footnote to Table S4). Divide the last column by 1.07 K (the population-weighted CO_2-induced temperature change from Table S4) to obtain the health effect per 1 K.

[b]USEPA and OEHHA cancers/yr were found by summing the product of individual CUREs (cancer unit risk estimates = increased 70-year cancer risk per $\mu g/m^3$ sustained concentration change) by the population-weighted mixing ratio or mixing ratio difference of a carcinogen, by the population, and air density, over all carcinogens, then dividing by 70 yr. USEPA CURES are 1.3×10^{-5} (formaldehyde), 2.2×10^{-6} (acetaldehyde), 3.0×10^{-5} (butadiene), 5.0×10^{-6} (= average of 2.2×10^{-6} and 7.8×10^{-6}) (benzene) (www.epa.gov/IRIS/). OEHHA CUREs are 6.0×10^{-6} (formaldehyde), 2.7×10^{-6} (acetaldehyde), 1.7×10^{-4} (butadiene), 2.9×10^{-5} (benzene) (www.oehha.ca.gov/risk/ChemicalDB/index.asp).

[c]8-hr ozone $\geq$35 ppbv is the highest 8-hour-averaged ozone during each day, averaged over all days of the four-month simulation in areas where this value $\geq$35 ppbv in the base case. When base $O_3 \geq$ 35 ppbv and no-fCO_2 O_3 < 35 ppbv, the mixing ratio difference was base O_3 minus 35 ppbv.

[d]The 2007 population exposed to $\geq$35 ppbv O_3 is the population exposed to a four-month-averaged 8-hour averaged ozone mixing ratio above 35 ppbv and was determined from the base case.

[e]High, medium, and low deaths/yr, hospitalizations/yr, and emergency-room (ER) visits/yr due to short-term O_3 exposure were obtained from Equation 2 applied to each model cell, summed over all cells. The baseline 2003 U.S. death rate (y_0) was 833 deaths/yr per 100,000 [Hoyert et al., 2006]. The baseline 2002 hospitalization rate due to respiratory problems was 1189 per 100,000 [Merrill and Elixhauser, 2005]. The baseline 1999 all-age emergency-room visit rate for asthma was 732 per 100,000 [Mannino et al., 2002]. These rates were assumed to be the same in each U.S. county, although they vary slightly by county. The fraction increases (b) in the number of deaths from all causes due to ozone were 0.006, 0.004, and 0.002 per 10 ppbv increase in daily 1-hr maximum ozone [Ostro et al., 2006]. These were multiplied by 1.33 to convert the risk associated with 10 ppbv increase in 1-hr maximum O_3 to that associated with a 10 ppbv increase in 8-hour average O_3 [Thurston and Ito, 2001]. The central value of the increased risk of hospitalization due to respiratory disease was 1.65% per 10 ppbv increase in 1-hour maximum O_3 (2.19% per 10 ppbv increase in 8-hour average O_3), and that for all-age ER visits for asthma was 2.4% per 10 ppbv increase in 1-hour O_3 [Ostro et al., 2006] (3.2% per 10 ppbv increase in 8-hour O_3). All values were reduced by 45% to account for the mid-July to mid-November and year-around $O_3 \geq$ 35 ppbv ratio, obtained from detailed observations (H. Tran, personal communication, 2007).

[f]This is the simulated 24-hr $PM_{2.5}$, averaged over four months, in locations where $PM_{2.5} \geq 0$ $\mu g/m^3$.

[g]The death rate due to long-term $PM_{2.5}$ exposure was calculated from Equation 2. Pope et al. [2002] provide increased dearth risks to those $\geq$30 years of 0.008 (high), 0.004 (medium), and 0.001 (low) per 1 $\mu g/m^3$ $PM_{2.5}$ >8 $\mu g/m^3$ based on 1979–1983 data. From 0–8 $\mu g/m^3$, the increased risks were conservatively but arbitrarily assumed = 1/4 those >8 $\mu g/m^3$ to account for reduced risk near zero $PM_{2.5}$. Assuming a higher risk would strengthen the conclusion found here. The all-cause 2003 U.S. death rate of those $\geq$30 years was 809.7 deaths/yr per 100,000 total population. No scaling of results from the 4-month model period to the annual average was performed to be conservative, since $PM_{2.5}$ concentrations from July–November are lower than in the annual average based on California data (H. Tran, personal communication, 2007).

increase from 1954–2000 [Rosenlof et al., 2001], but a slight lower-stratospheric decrease from 2001–2005 [Randel et al., 2006]. The simulations here, which accounted for chlorine and bromine gas and heterogeneous chemistry, found that the temperature and H_2O changes due to fCO_2 increased middle and upper-stratospheric ozone but decreased upper tropospheric and lower stratospheric (UTLS) ozone, where its column abundance is greater, causing a net U.S. column ozone loss of 2.7% (Figure 2c, ii, and Table S4). The UTLS ozone losses were due to increases in H_2O there (Figure 2b, ii), as indicated by Figure S2b and Dvortsov and Solomon [2001]. The upper- and middle-stratospheric gains can be explained by Figure S1, which shows that, at 25 km, stratospheric ozone decreases by 1.5% as H_2O increases by 1 ppmv. As temperature decreases by 1.5 K, though, ozone increases by 3.6%, suggesting an overall ozone increase from H_2O and cooling. The ozone increase upon stratospheric cooling is due to reduced loss from $O+O_3$ [Evans et al., 1998]. Despite the column ozone loss due to fCO_2, surface UV hardly changed (Table S4) because fCO_2 increased cloud optical depth, offsetting UV increases from ozone loss.

5. Summary

[19] A climate-air pollution model showed by cause and effect that fossil-fuel CO_2 increases increase U.S. surface ozone, carcinogens, and particulate matter, thereby increasing death, asthma, hospitalization, and cancer rates. Increased water vapor and temperatures due to higher CO_2

each increase ozone increasingly with increasing ozone. At low ozone, more water vapor decreases ozone slightly but higher temperatures increase biogenic emission in many areas, offsetting ozone decreases in such areas. CO_2 increases stability, the relative humidity, and biogenic particle mass thus $PM_{2.5}$. Finally, CO_2 decreases column ozone over the U.S. by increasing upper tropospheric/lower stratospheric water vapor.

[20] Acknowledgments. NASA grants NNG04GE93G and NNG04GJ89G and U.S. Environmental Protection Agency grant RD-83337101-O. I thank Hien Tran of the California Air Resources Board for helpful health statistic comments.

References

Aw, J., and M. J. Kleeman (2003), Evaluating the first-order effect of intraannual temperature variability on urban air pollution, J. Geophys. Res., 108(D12), 4365, doi:10.1029/2002JD002688.

Brasseur, G. P., M. M. Schultz, C. Granier, M. Saunois, T. Diehl, M. Botzet, and E. Roeckner (2006), Impact of climate change on the future chemical composition of the global troposphere, J. Clim., 19, 3932–3951.

Colella, W. G., M. Z. Jacobson, and D. M. Golden (2005), Switching to a U. S. hydrogen fuel cell vehicle fleet: The resultant change in emissions, energy use, and greenhouse gases, J. Power Sources, 150, 150–181.

Dvortsov, V. L., and S. Solomon (2001), Response of the stratospheric temperatures and ozone to past and future increases in stratospheric humidity, J. Geophys. Res., 106, 7505–7514.

Evans, S. J., R. Toumi, J. E. Harries, M. P. Chipperfield, and J. M. Russell III (1998), Trends in stratospheric humidity and the sensitivity of ozone to these trends, J. Geophys. Res., 103, 8715–8725.

Gaffen, D. J., and R. J. Ross (1999), Climatology and trends of U.S. surface humidity and temperature, J. Clim., 12, 811–828.

Guenther, A., et al. (1995), A global model of natural volatile organic compound emissions, J. Geophys. Res., 100, 8873–8892.

Hoyert, D. L., M. P. Heron, S. L. Murphy, and H.-C. Kung, (2006), National vital statistics, Rep. 54 (13), Cent. for Disease Control and Prev., Hyattsville, Md. (Available at http://www.cdc.gov/nchs/fastats/deaths.htm)

Intergovernmental Panel on Climate Change (2001), Climate Change 2001: The Scientific Basis, edited by J. T. Houghton et al., Cambridge Univ. Press, New York.

Jacobson, M. Z. (2001), GATOR-GCMM: 2. A study of day- and nighttime ozone layers aloft, ozone in national parks, and weather during the SARMAP Field Campaign, J. Geophys. Res., 106, 5403–5420.

Jacobson, M. Z. (2007), Effects of ethanol versus gasoline on cancer and mortality in the United States, Environ. Sci. Technol., 41, 4150–4157, doi:10.1021/es062085v.

Jacobson, M. Z., J. H. Seinfeld, G. R. Carmichael, and D. G. Streets (2004), The effect on photochemical smog of converting the U. S. fleet of gasoline vehicles to modern diesel vehicles, Geophys. Res. Lett., 31, L02116, doi:10.1029/2003GL018448.

Jacobson, M. Z., Y. J. Kaufmann, and Y. Rudich (2007), Examining feedbacks of aerosols to urban climate with a model that treats 3-D clouds with aerosol inclusions, J. Geophys. Res., 112, D24205, doi:10.1029/2007JD008922.

Liao, H., W.-T. Chen, and J. H. Seinfeld (2006), Role of climate change in global predictions of future tropospheric ozone and aerosols, J. Geophys. Res., 111, D12304, doi:10.1029/2005JD006852.

Mannino, D. M., D. M. Homa, L. J. Akinbami, J. E. Moorman, C. Gwynn, and S. C. Redd (2002), Surveillance for asthma: United States, 1980–1990, Morbidity Mortality Weekly Rep. Surveillance Summaries 51 (SS01), pp. 1–13, Cent. for Disease Control, Atlanta, Ga.

Medina-Ramon, M., and J. Schwartz (2007), Temperature, temperature extremes, and mortality: A study of acclimatization and effect modification in 50 U.S. cities, Occup. Environ. Med., 64, 827–833, doi:10.1136/oem.2007.033175.

Merrill, C. T., and A. Elixhauser (2005), Appendix, in Hospitalization in the United States, 2002, HCUP Fact Book 6, Agency for Healthcare Res. and Qual., Rockville, Md. (Available at www.ahrq.gov/data/hcup/factbk6/factbk6e.htm)

Mickley, L. J., D. J. Jacob, B. D. Field, and D. Rind (2004), Effects of future climate change on regional air pollution episodes in the United States, Geophys. Res. Lett., 31, L24103, doi:10.1029/2004GL021216.

Murazaki, K., and P. Hess (2006), How does climate change contribute to surface ozone change over the United States?, J. Geophys. Res., 111, D05301, doi:10.1029/2005JD005873.

Olszyna, K. J., M. Luria, and J. F. Meagher (1997), The correlation of temperature and rural ozone levels in southeastern U.S.A., Atmos. Environ., 31, 3011–3022.

Ostro, B. D., H. Tran, and J. I. Levy (2006), The health benefits of reduced tropospheric ozone in California, J. Air Waste Manage. Assoc., 56, 1007–1021.

Pope, C. A., III, R. T. Burnett, M. J. Thun, E. E. Calle, D. Krewski, K. Ito, and G. D. Thurston (2002), Lung cancer, cardiopulmonary mortality, and long-term exposure to fine particulate air pollution, J. Am. Med. Assoc., 287, 1132–1141.

Racherla, P. N., and P. J. Adams (2006), Sensitivity of global tropospheric ozone and fine particulate matter concentrations to climate change, J. Geophys. Res., 111, D24103, doi:10.1029/2005JD006939.

Randel, W. J., F. Wu, H. Vömel, G. E. Nedoluha, and P. Forster (2006), Decreases in stratospheric water vapor after 2001: Links to changes in the tropical tropopause and the Brewer-Dobson circulation, J. Geophys. Res., 111, D12312, doi:10.1029/2005JD006744.

Rosenlof, K. H., et al. (2001), Stratospheric water vapor increases over the past half-century, Geophys. Res. Lett., 28, 1195–1198.

Rubin, J. I., A. J. Kean, R. A. Harley, D. B. Millet, and A. H. Goldstein (2006), Temperature dependence of volatile organic compound evaporative emissions from motor vehicles, J. Geophys. Res., 111, D03305, doi:10.1029/2005JD006458.

Sillman, S., and P. J. Samson (1995), Impact of temperature on oxidant photochemistry in urban, polluted rural, and remote environments, J. Geophys. Res., 100, 11,497–11,508.

Steiner, A. L., S. Tonse, R. C. Cohen, A. H. Goldstein, and R. A. Harley (2006), Influence of future climate and emissions on regional air quality in California, J. Geophys. Res., 111, D18303, doi:10.1029/2005JD006935.

Stevenson, D., R. Doherty, M. Sanderson, C. Johnson, B. Collins, and D. Derwent (2005), Impacts of climate change and variability on tropospheric ozone and its precursors, Faraday Discuss., 130, 1–17.

Thompson, A. M., R. W. Stewart, M. A. Owens, and J. A. Herwehe (1989), Sensitivity of tropospheric oxidants to global chemical and climate change, Atmos. Environ., 23, 519–532.

Thorne, P. W., D. E. Parker, S. F. B. Tett, P. D. Jones, M. McCarthy, H. Coleman, and P. Brohan (2005), Revisiting radiosonde upper-air temperatures from 1958 to 2002, J. Geophys. Res., 110, D18105, doi:10.1029/2004JD005753.

Thurston, G. D., and K. Ito (2001), Epidemiological studies of acute ozone exposures and mortality, J. Exposure Anal. Environ. Epidemiology, 11, 286–294.

Unger, N., D. T. Shindell, D. M. Koch, M. Amann, J. Cofala, and D. G. Streets (2006), Influences of man-made emissions and climate changes on tropospheric ozone, methane, and sulfate at 2030 from a broad range of possible futures, J. Geophys. Res., 111, D12313, doi:10.1029/2005JD006518.

West, J. J., A. M. Fiore, L. W. Horowitz, and D. L. Mauzerall (2006), Global health benefits of mitigating ozone pollution with methane emission controls, Proc. Natl. Acad. Sci. U. S. A., 103, 3988–3993.

Zhang, Y., C. H. Bischof, R. C. Easter, and P.-T. Wu (1998), Sensitivity analysis of a mixed phase chemical mechanism using automatic differentiation, J. Geophys. Res., 103, 18,953–18,797.

M. Z. Jacobson, Department of Civil and Environmental Engineering, Stanford University, Stanford, CA 94305-4020, USA. (jacobson@stanford.edu)

Attachment 2 of 2 to
Email 5 of 11

Environ. Sci. Technol. **2010,** *44,* 2497–2502

Enhancement of Local Air Pollution by Urban CO_2 Domes

MARK Z. JACOBSON*

Department of Civil and Environmental Engineering, Stanford University, Stanford, California 94305-4020

Received October 3, 2009. Revised manuscript received December 21, 2009. Accepted March 2, 2010.

Data suggest that domes of high CO_2 levels form over cities. Despite our knowledge of these domes for over a decade, no study has contemplated their effects on air pollution or health. In fact, all air pollution regulations worldwide assume arbitrarily that such domes have no local health impact, and carbon policy proposals, such as "cap and trade", implicitly assume that CO_2 impacts are the same regardless of where emissions occur. Here, it is found through data-evaluated numerical modeling with telescoping domains from the globe to the U.S., California, and Los Angeles, that local CO_2 emissions in isolation may increase local ozone and particulate matter. Although health impacts of such changes are uncertain, they are of concern, and it is estimated that that local CO_2 emissions may increase premature mortality by 50−100 and 300−1000/yr in California and the U.S., respectively. As such, reducing locally emitted CO_2 may reduce local air pollution mortality even if CO_2 in adjacent regions is not controlled. If correct, this result contradicts the basis for air pollution regulations worldwide, none of which considers controlling local CO_2 based on its local health impacts. It also suggests that a "cap and trade" policy should consider the location of CO_2 emissions, as the underlying assumption of the policy is incorrect.

Introduction

Although CO_2 is generally well-mixed in the atmosphere, data indicate that its mixing ratios are higher in urban than in background air, resulting in *urban CO_2 domes* (*1–6*). Measurements in Phoenix, for example, indicate that peak and mean CO_2 in the city center were 75% and 38−43% higher, respectively, than in surrounding rural areas (*2*). Recent studies have examined the impact of global greenhouse gases on air pollution (*7–13*). Whereas one study used a 1-D model to estimate the temperature profile impact of a CO_2 dome (*3*), no study has isolated the impact of locally emitted CO_2 on air pollution or health. One reason is that model simulations of such an effect require treatment of meteorological feedbacks to gas, aerosol, and cloud changes, and few models include such feedbacks in detail. Second, local CO_2 emissions are close to the ground, where the temperature contrast between the Earth's surface and the lowest CO_2 layers is small. However, studies have not considered that CO_2 domes result in CO_2 gradients high above the surface. If locally emitted CO_2 increases local air pollution, then cities, counties, states, and small countries can reduce air pollution health problems by reducing their own CO_2 emissions, regardless of whether other air pollutants are reduced locally or whether other locations reduce CO_2.

* Corresponding author phone: (650)723-6836; e-mail: jacobson@stanford.edu.

Methodology and Evaluation

For this study, the nested global-through-urban 3-D model, GATOR-GCMOM (*13–17*) was used to examine the effects of locally emitted CO_2 on local climate and air pollution. A nested model is one that telescopes from a large scale to more finely resolved domains. The model and its feedbacks are described in the Supporting Information. Example CO_2 feedbacks treated include those to heating rates thus temperatures, which affect (a) local temperature and pressure gradients, stability, wind speeds, cloudiness, and gas/particle transport, (b) water evaporation rates, (c) the relative humidity and particle swelling, and (d) temperature-dependent natural emissions, air chemistry, and particle microphysics. Changes in CO_2 also affect (e) photosynthesis and respiration rates, (f) dissolution and evaporation rates of CO_2 into the ocean, (g) weathering rates, (h) ocean pH and chemical composition, (i) sea spray pH and composition, and (j) rainwater pH and composition. Changes in sea spray composition, in turn, affect sea spray radiative properties, thus heating rates.

The model was nested from the globe (resolution 4°SN×5°WE) to the U.S. (0.5°×0.75°), California (0.20°×0.15°), and Los Angeles (0.045°×0.05°). The global domain included 47 sigma-pressure layers up to 0.22 hPa (∼60 km), with high resolution (15 layers) in the bottom 1 km. The nested regional domains included 35 layers exactly matching the global layers up to 65 hPa (∼18 km). The model was initialized with 1-degree global reanalysis data (*18*) but run without data assimilation or model spinup.

Three original pairs of baseline and sensitivity simulations were run: one pair nested from the globe to California for one year (2006), one pair nested from the globe to California to Los Angeles for two sets of three months (Feb-Apr, Aug-Oct, 2006), and one pair nested from the globe to the U.S. for two sets of three months (Jan-Mar, Jul-Sep, 2006). The seasonal periods were selected to obtain roughly winter/summer results that could be averaged to estimate annual values. A second 1-year (2007) simulation pair was run for California to test interannual variability. In each sensitivity simulation, only anthropogenic CO_2 emissions ($emCO_2$) were removed from the finest domain. Initial ambient CO_2 was the same in all domains of both simulations, and $emCO_2$ was the same in the parent domains of both. As such, all resulting differences were due solely to initial changes in locally emitted (in the finest domain) CO_2.

The model and comparisons with data have been described in over 50 papers, including recently (*13–17*). Figure 1 further compares modeled O_3, PM_{10}, and CH_3CHO from August 1−7 of the baseline (with $emCO_2$) and sensitivity (no $emCO_2$) simulations from the Los Angeles domain with data. The comparisons indicate good agreement for ozone in particular. Since $emCO_2$ was the only variable that differed initially between simulations, it was the initiating causal factor in the increases in O_3, PM_{10}, and CH_3CHO seen in Figure 1. Although ozone was predicted slightly better in the no-$emCO_2$ case than in the $emCO_2$ case during some hours, modeled ozone in the $emCO_2$ case matched peaks better by about 0.5% averaged over comparisons with all data shown and not shown.

Results

Figure 2a,b shows the modeled contribution of California's CO_2 emissions to surface and column CO_2, respectively, averaged over a year. The CO_2 domes over Los Angeles, the San Francisco Bay Area, Sacramento (38.58 N, 121.49 W),

10.1021/es903018m
Published on Web 03/10/2010

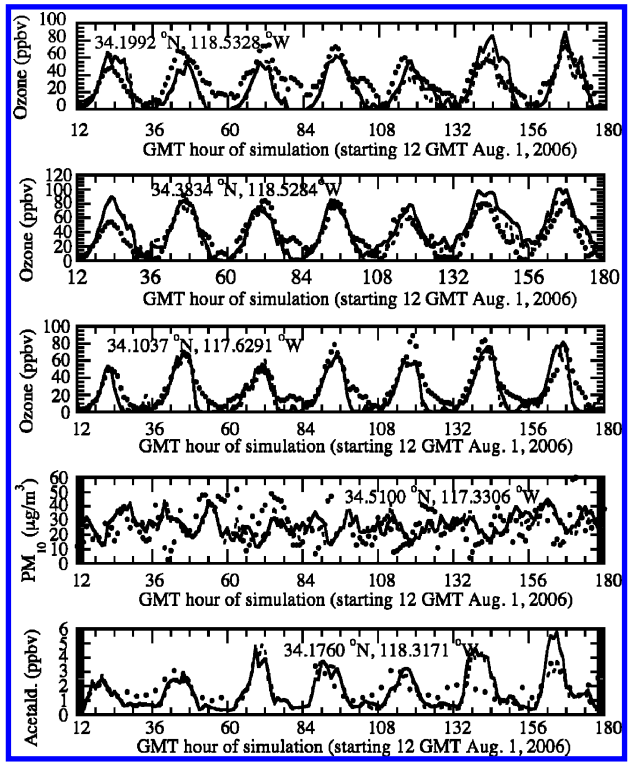

FIGURE 1. Paired-in-time-and-space comparisons of modeled baseline (solid lines), modeled no-emCO_2 (dashed lines), and data (22) (dots) for ozone, sub-10-μm particle mass, and acetaldehyde from the Los Angeles domain for August 1−7, 2006 of the Aug-Oct 2006 simulation. Local standard time is GMT minus 8 h.

and the Southern Central Valley are evident. The largest surface CO_2 increase (5%, or 17.5 ppmv) was lower than observed increases in cities (*2*) since the resolution of the California domain was coarser than the resolution of measurements. As shown below for Los Angeles, an increase in model resolution increases the magnitude of the surface and column CO_2 dome.

Population-weighted (PW) and domain-averaged (DA) changes in several parameters can help to elucidate the effects of the CO_2 domes. A PW value is the product of a parameter value and population in a grid cell, summed over all grid cells, all divided by the summed population among all cells. Thus, a PW value indicates changes primarily in populated areas, whereas a DA value indicates changes everywhere, independent of population. The PW and DA increases in surface CO_2 due to emCO_2 were 7.4 ppmv and 1.3 ppmv, respectively, but the corresponding increases in column CO_2 were 6.0 g/m^2 and 1.53 g/m^2, respectively, indicating, along with Figure 2a,b, that changes in column CO_2 were spread horizontally more than were changes in surface CO_2. This is because surface winds are usually slower than winds aloft, so only when surface CO_2 mixes vertically is it transported much horizontally, and when that occurs, surface CO_2 is quickly replenished with new emissions.

The CO_2 increases in California increased the PW air temperature by about 0.0063 K, more than it changed the domain-averaged air temperature (+0.00046) (Figure 2c). Thus, CO_2 domes had greater temperature impacts where the CO_2 was emitted and where people lived than in the domain average. This result held for the effects of emCO_2 on column water vapor (Figure 2d - PW: +4.3 g/m^2; DA: +0.88 g/m^2), ozone (Figure 2e - PW: +0.06 ppbv; DA: +0.0043 ppbv), $PM_{2.5}$ (Figure 2g - PW: +0.08 μg/m^3; DA: −0.0052 μg/m^3), and PAN (Figure 2i - PW: +0.002 ppbv; DA: −0.000005 ppbv). The peak surface air temperature increases in Figure 2c (and in the Los Angeles simulations) were ~0.1 K, similar to those found from 1-D radiative only calculations for Phoenix (*3*). Peak ozone and its health effects occurred over Los Angeles and Sacramento (Figure 2e,f), where increases in CO_2 (Figure 2a), temperature (although small for Sacramento, Figure 2c), and column H_2O (Figure 2d) occurred.

Figure 3 elucidates spatial correlations between annually averaged changes in local ambient CO_2 caused by emCO_2 and changes in other parameters. Increases in temperature, water vapor, and ozone correlated positively and with statistical significance ($p << 0.05$) with increases in CO_2. Ozone increases also correlated positively and with strong significance with increases in water vapor and temperature. A previous study found that increases in temperature and water vapor both increase ozone at high ozone but cause little change in ozone at low ozone (*13*), consistent with this result.

$PM_{2.5}$ correlated slightly negatively ($r = 0.017$) but without statistical significance, with higher temperature and much more positively ($r = 0.23$) and with strong significance ($p < 0.0001$) with higher water vapor in California. Higher temperature decreased $PM_{2.5}$ by increasing vapor pressures thus PM evaporation and by enhancing precipitation in some locations. Some $PM_{2.5}$ decreases with higher temperature were offset by biogenic organic emission increases with higher temperatures followed by biogenic oxidation to organic PM. But, in populated areas of California, biogenic emissions are relatively low. Some $PM_{2.5}$ decreases were also offset by surface $PM_{2.5}$ increases caused by slower surface winds due to enhanced boundary-layer stability from CO_2, which reduced the downward transport of fast winds aloft to the surface (*13*). While higher temperature slightly decreased $PM_{2.5}$, higher water vapor due to emCO_2 increased $PM_{2.5}$ by increasing aerosol water content, increasing nitric acid and ammonia gas dissolution, forming more particle nitrate and ammonium. Higher ozone from higher water vapor also increased oxidation of organic gases to organic PM. Overall, $PM_{2.5}$ increased with increasing CO_2, but because of the opposing effects of temperature and water vapor on $PM_{2.5}$, the net positive correlation was weak ($r = 0.022$) and not statistically significant ($p = 0.17$). However, when all CO_2 increases below 1 ppmv were removed, the correlation improved substantially ($r = 0.047$, $p = 0.07$). Further, the correlation was strongly statistically significant for Los Angeles and U.S. domains, as discussed shortly.

Health effect rates (y) due to pollutants in each model domain for each simulation were determined from

$$y = y_0 \sum_i \left\{ P_i \sum_t (1 - \exp[-\beta \times \max(x_{i,t} - x_{th}, 0)]) \right\} \quad (1)$$

where $x_{i,t}$ is the concentration in grid cell i at time t, x_{th} is the threshold concentration below which no health effect occurs, β is the fractional increase in risk per unit x, y_0 is the baseline health effect rate, and P_i is the grid cell population. Table 1 provides sums or values of P, β, y_0, and x_{th}. Differences in health effects between two simulations were obtained by differencing the aggregated effects from each simulation determined from eq 1. The relationship between ozone exposure and premature mortality is uncertain; however, ref *19* suggests that it is "highly unlikely" to be zero. Similarly, ref *20* suggests that the exact relationship between $PM_{2.5}$ exposure and mortality is uncertain but "likely causal". Cardiovascular effects of $PM_{2.5}$ are more strongly "causal". Although health effects of $PM_{2.5}$ differ for different chemical components within $PM_{2.5}$, almost all epidemiological studies

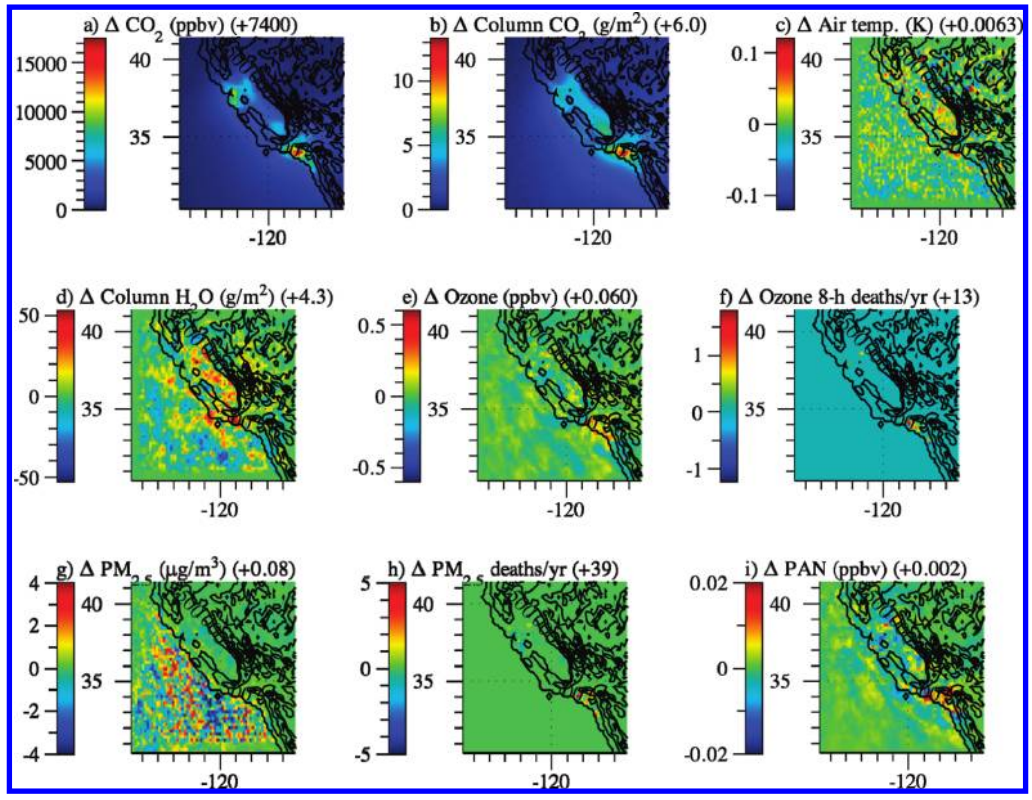

FIGURE 2. Modeled annually averaged difference for several surface or column (if indicated) parameters in California, parts of Nevada, and parts of New Mexico when two simulations (with and without emCO_2) were run. The numbers in parentheses are average population-weighted changes for the domain shown.

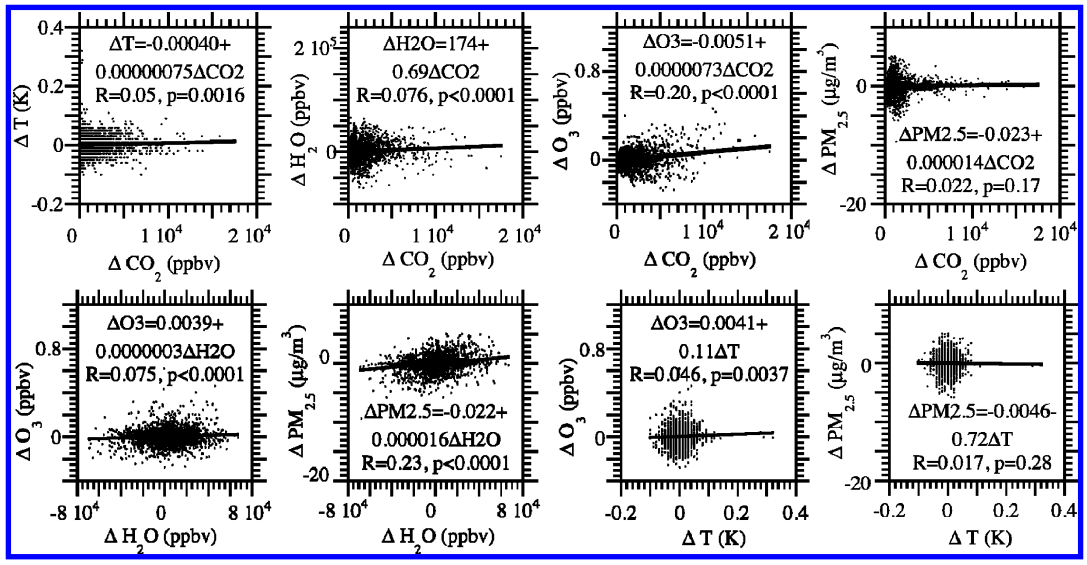

FIGURE 3. Scatter plots of paired-in-space one-year-averaged changes between several parameter pairs, obtained from all near-surface grid cells of the California domain. Also shown is an equation for the linear fit through the data points in each case and the *r* and *p* values for the fits. The equation describes correlation only, not cause and effect, between each parameter pair.

correlating particle changes with health use ambient $PM_{2.5}$ measurements to derive such correlations. For consistency, it is therefore necessary to apply β values from such studies to modeled $PM_{2.5}$ (*22*).

California's local CO_2 resulted here in ~13 (with a range of 6−19 due to uncertainty in epidemiological data) additional ozone-related premature mortalities/year (Figure 2f) or 0.3% above the baseline 4600 (2300−6900)/year (Table 1). Higher $PM_{2.5}$ due to emCO_2 contributed another ~39 (13−60) premature mortalities/year (Figure 2h), 0.2% above the baseline rate of 22,500 (5900−42,000)/year. Changes in cancer due to emCO_2 were relatively small (Table 1). Additional uncertainty arises due to the model itself and interannual variations in concentration. Some of the model uncertainties are elucidated in comparisons with data, such as in Figure 1; however, it is difficult to translate such uncertainty into mortality uncertainty. Interannual variations in concentrations were examined by running a second pair of simulations for California, starting one year after the first. The results of this simulation

TABLE 1. Summary of Locally-Emitted CO_2's ($emCO_2$) Effects on Cancer, Ozone Mortality, Ozone Hospitalization, Ozone Emergency-Room (ER) Visits, and Particulate-Matter Mortality in California (CA), Los Angeles (LA), and the United States (U.S.)[d]

	annual base CA	base minus no $emCO_2$CA	annual base LA	base minus no $emCO_2$ LA	annual base U.S.	base minus no $emCO_2$ U.S.
ozone ≥ 35 ppbv (ppbv)	47.4	+0.060	44.7	+0.12	47.0	+0.044
$PM_{2.5}$ ($\mu g/m^3$) (pop-weight)	50.0	+0.08	36	+0.29	64.4	+0.041
$PM_{2.5}$ ($\mu g/m^3$) (all land)	21.5	−0.007	25.8	+0.06	32.8	+0.039
formaldehyde (ppbv)	4.43	+0.0030	4.1	+0.054	6.75	+0.066
acetaldehyde (ppbv)	1.35	+0.0017	1.3	+0.021	2.45	+0.016
1,3-butadiene (ppbv)	0.11	−0.00024	0.23	+0.0020	0.077	+0.0005
benzene (ppbv)	0.30	−0.00009	0.37	+0.0041	0.34	+0.020
			Cancer			
USEPA cancers/yr[a]	44.1	0.016	22.0	+0.28	573	+6.9
OEHHA cancers/yr[a]	54.4	−0.038	37.8	+0.39	561	+11.8
			Ozone Health Effects			
high O_3 mortalities/yr[b]	6860	+19	2140	+20	52,300	+245
med. O_3 mortalities/yr[b]	4600	+13	1430	+14	35,100	+166
low O_3 mortalities/yr[b]	2300	+6	718	+7	17,620	+85
O_3 hospitalizations/yr[b]	26,300	+65	8270	+75	200,000	+867
ozone ER visits/yr[b]	23,200	+56	7320	+66	175,000	+721
			PM Health Effects			
high $PM_{2.5}$ mortalities/yr[c]	42,000	+60	16,220	+147	44,800	+810
med. $PM_{2.5}$ mortalities/yr[c]	22,500	+39	8500	+81	169,000	+607
low $PM_{2.5}$ mortalities/yr[c]	5900	+13	2200	+22	316,000	+201

[a] USEPA (U.S. Environmental Protection Agency) and OEHHA (Office of Environmental Health Hazard Assessment) cancers/yr were found by summing, over all model surface grid cells and the four carcinogens (formaldehyde, acetaldehyde, 1,3-butadiene, and benzene), the product of individual CUREs (cancer unit risk estimates=increased 70-year cancer risk per $\mu g/m^3$ sustained concentration change), the mass concentration ($\mu g/m^3$) (for baseline statistics) or mass concentration difference (for difference statistics) of the carcinogen, and the population in the cell and then dividing by the population of the model domain and by 70 yr. USEPA CURES were 1.3×10^{-5} (formaldehyde), 2.2×10^{-6} (acetaldehyde), 3.0×10^{-5} (butadiene), 5.0×10^{-6} (=average of 2.2×10^{-6} and 7.8×10^{-6}) (benzene) (www.epa.gov/IRIS/). OEHHA CUREs were 6.0×10^{-6} (formaldehyde), 2.7×10^{-6} (acetaldehyde), 1.7×10^{-4} (butadiene), 2.9×10^{-5} (benzene) (www.oehha.ca.gov/risk/ChemicalDB/index.asp). [b] High, medium, and low mortalities/yr, hospitalizations/yr, and emergency-room (ER) visits/yr due to short-term O_3 exposure were obtained from eq 1, assuming a threshold (x_{th}) of 35 ppbv (*23*). The baseline 2003 U.S. mortality rate (y_0) was 833 mortalities/yr per 100,000 (*24*). The baseline 2002 hospitalization rate due to respiratory problems was 1189 per 100,000 (*25*). The baseline 1999 all-age emergency-room visit rate for asthma was 732 per 100,000 (*26*). The fractional increases (β) in the number of premature mortalities from all causes due to ozone were 0.006, 0.004, and 0.002 per 10 ppbv increase in daily 1-h maximum ozone (*27*). These were multiplied by 1.33 to convert the risk associated with a 10 ppbv increase in 1-h maximum O_3 to that associated with a 10 ppbv increase in 8-h average O_3 (*23*). The central value of the increased risk of hospitalization due to respiratory disease was 1.65% per 10 ppbv increase in 1-h maximum O_3 (2.19% per 10 ppbv increase in 8-h average O_3), and that for all-age ER visits for asthma was 2.4% per 10 ppbv increase in 1-h O_3 (3.2% per 10 ppbv increase in 8-h O_3) (*25, 26*). [c] The mortality rate due to long-term PM_{25} exposure was calculated from eq 1. Increased premature mortality risks to those ≥30 years were 0.008 (high), 0.004 (medium), and 0.001 (low) per 1 $\mu g/m^3$ $PM_{2.5} > 8$ $\mu g/m^3$ based on 1979−1983 data (*28*). From 0−8 $\mu g/m^3$, the increased risks were assumed to be a quarter of the risks for those >8 $\mu g/m^3$ to account for reduced risk near zero $PM_{2.5}$ (*13*). The all-cause 2003 U.S. mortality rate of those ≥30 years was 809.7 mortalities/yr per 100,000 total population. Reference *29* provides higher relative risks of $PM_{2.5}$ health effects data; however, the values from ref *28* were retained to be conservative. [d] Results are shown for the with-$emCO_2$ emissions simulation ("base") and the difference between the base and no $emCO_2$ emissions simulations ("base minus no-$emCO_2$") for each case. The domain summed populations (sum of P_i in eq 1) in the CA, LA, and U.S. domains were 35.35 million, 17.268 million, and 324.07 million, respectively. All concentrations except the second $PM_{2.5}$, which is an all-land average, were near-surface values weighted spatially by population. $PM_{2.5}$ concentrations in the table include liquid water, but $PM_{2.5}$ used for health calculations were dry. CA results were for an entire year, LA results were an average of Feb-Apr and Aug-Oct (Figure 4), and U.S. results were an average of Jan-Mar and Jul-Sep.

were similar to those for the first, with ~51 (17−82) additional ozone- plus $PM_{2.5}$ -related premature mortalities/year attributable to $emCO_2$.

Simulations for Los Angeles echo results for California but allowed for a more resolved picture of the effects of $emCO_2$. Figure 4a (Feb-Apr) indicates that the near-surface CO_2 dome that formed over Los Angeles peaked at about 34 ppmv, twice that over the coarser California domain. The column difference (Figure 4b) indicates a spreading of the dome over a larger area than the surface dome. In Feb-Apr and Aug-Oct, $emCO_2$ enhanced PW ozone and $PM_{2.5}$, increasing mortality (Figure 4, Table 1) and other health effects (Table 1). The causes of such increases, however, differed with season.

During Feb-Apr, infrared absorption by $emCO_2$ warmed air temperatures (Figure 4c) up to ~3 km altitude, increasing the land-ocean temperature gradient by about 0.2 K over 50 km, increasing surface sea-breeze wind speeds by ~0.06 m/s, and increasing water vapor transport to and soil−water evaporation in Los Angeles (Figure 4d). Higher temperatures and water vapor slightly increased ozone and $PM_{2.5}$ for the reasons given in ref *13*. The high wind speeds also increased resuspension of road and soil dust and moved PM more to the eastern basin.

During summer, Los Angeles boundary layer heights, temperature inversions, land-sea temperature gradients, sea breeze wind speeds, water evaporation rates, column water vapor, and stratus cloud formation are greater than in summer. Since boundary-layer heights were higher during the Aug-Oct simulations, CO_2 mixed faster up to higher altitudes during summer. Initially, the higher CO_2 warmed the air up to 4 km above topography, but the higher

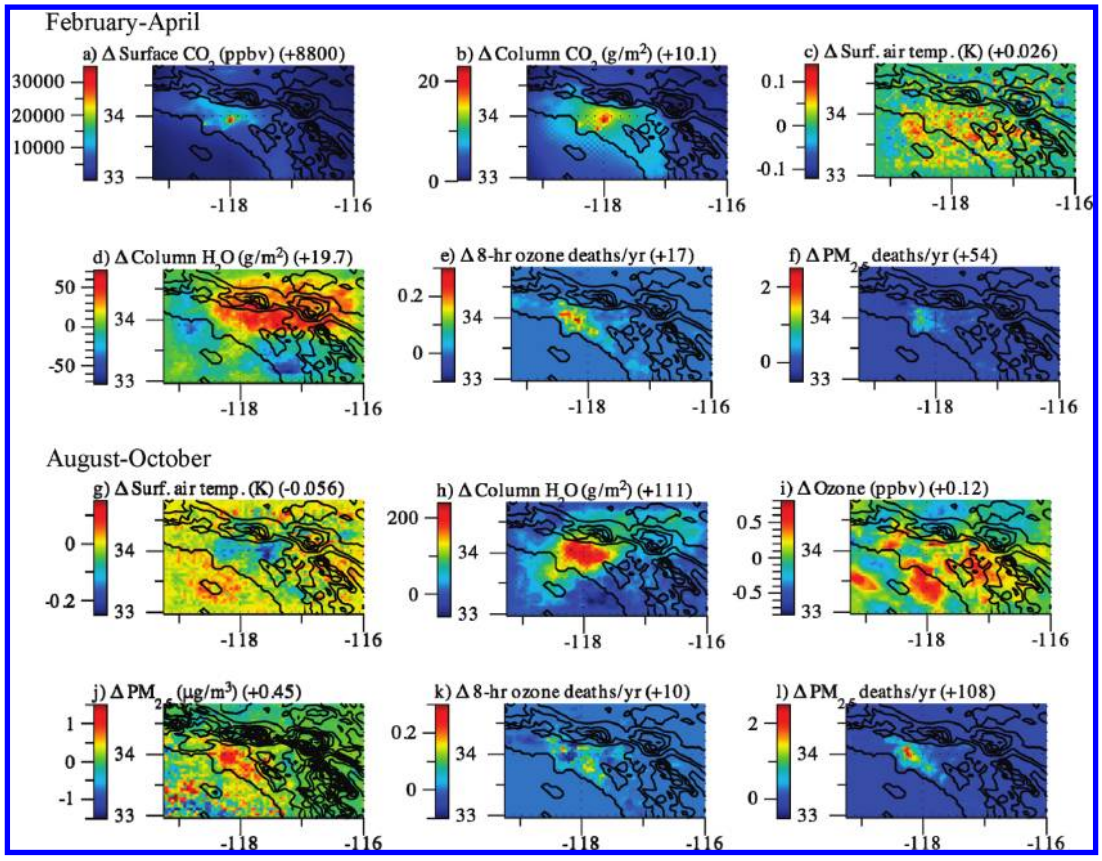

FIGURE 4. Same as Figure 2 but for the Los Angeles domain and for Feb-Apr and Aug-Oct.

temperatures from 1.5−4 km decreased the upper-level sea-breeze return flow (figures not shown) decreased pressure aloft, reducing the flow of moisture from land to ocean aloft (increasing it from ocean to land), increasing cloud optical depth over land by up to 0.4−0.6 optical depth units, decreasing summer surface solar radiation by at most 3−4 W/m^2 locally, decreasing local ground temperatures by up to 0.2 K (Figure 4g) while retaining the warmer air aloft. The excess water vapor aloft over land mixed to the surface (Figure 4h), increasing ozone (which increases chemically with water vapor at high ozone) and the relative humidity, which increased aerosol particle swelling, increasing gas growth onto aerosols, and reducing particle evaporation. In summary, emCO_2 increased ozone and $PM_{2.5}$ and their corresponding health effects in both seasons, increasing air pollution mortality in California and Los Angeles by about 50−100 per year (Figure 4e,f,i,j, Table 1). The spatial positive correlations between increases in near-surface CO_2 and near-surface O_3 and $PM_{2.5}$ were both visually apparent (Figure 4) and strongly statistically significant (e.g., Aug-Oct, $r = 0.14$, $p < 0.0001$ for ΔCO_2 vs ΔO_3; $r = 0.24$, $p < 0.0001$ for ΔCO_2 vs $\Delta PM_{2.5}$).

For the U.S. as a whole, the correlations between increases in CO_2 and increases in O_3 and $PM_{2.5}$ premature mortality were also both visually apparent (Figure 5) and statistically significant ($r = 0.31$, $p < 0.0001$ for ΔCO_2 vs ΔO_3 mortality; $r = 0.32$, $p < 0.0001$ for ΔCO_2 vs $\Delta PM_{2.5}$ mortality). The Jun-Aug correlation between ΔCO_2 and $\Delta PM_{2.5}$ concentration ($r = 0.1$, $p < 0.0001$) was weaker than that between ΔCO_2 and $\Delta PM_{2.5}$ mortality, since local CO_2 fed back to meteorology, which fed back to $PM_{2.5}$ outside of cities as well as in cities, but few people were exposed to such changes in $PM_{2.5}$ outside of cities. Nevertheless, both correlations were strongly statistically significant.

The annual premature mortality rates due to emCO_2 in the U.S. were ~770 (300−1000), with ~20% due to ozone. This rate represented an enhancement of ~0.4% of the baseline mortality rate due to air pollution. With a U.S. anthropogenic emission rate of 5.76 GT-CO_2/yr (Table S2), this corresponds to ~134 (52−174) additional premature mortalities/GT-CO_2/yr over the U.S. Modeled mortality rates in Los Angeles for the Los Angeles domain were higher than those for Los Angeles in the California or U.S. domains due to the higher resolution of the Los Angeles domain; thus, mortality estimates for California and the U.S. may be low.

Implications

Worldwide, emissions of NO_x, HCs, CO, and PM are regulated. The few CO_2 regulations proposed to date have been justified based on its large-scale feedback to temperatures, sea levels, water supply, and global air pollution. No proposed CO_2 regulation is based on the potential impact of locally emitted CO_2 on local pollution as such effects have been assumed not to exist (*21*). Here, it was found that local CO_2 emissions can increase local ozone and particulate matter due to feedbacks to temperatures, atmospheric stability, water vapor, humidity, winds, and precipitation. Although modeled pollution changes and their health impacts are uncertain, results here suggests that reducing local CO_2 may reduce 300−1000 premature air pollution mortalities/yr in the U.S. and 50−100/yr in California, even if CO_2 in adjacent regions is not controlled. Thus, CO_2 emission controls may be justified on the same grounds that NO_x, HC, CO, and PM emission regulations are justified. Results further imply that the assumption behind the "cap and trade" policy, namely that CO_2 emitted in one location has the same impact as CO_2 emitted in another, is incorrect, as CO_2 emissions in populated cities have larger health impacts than CO_2 emissions in unpopulated

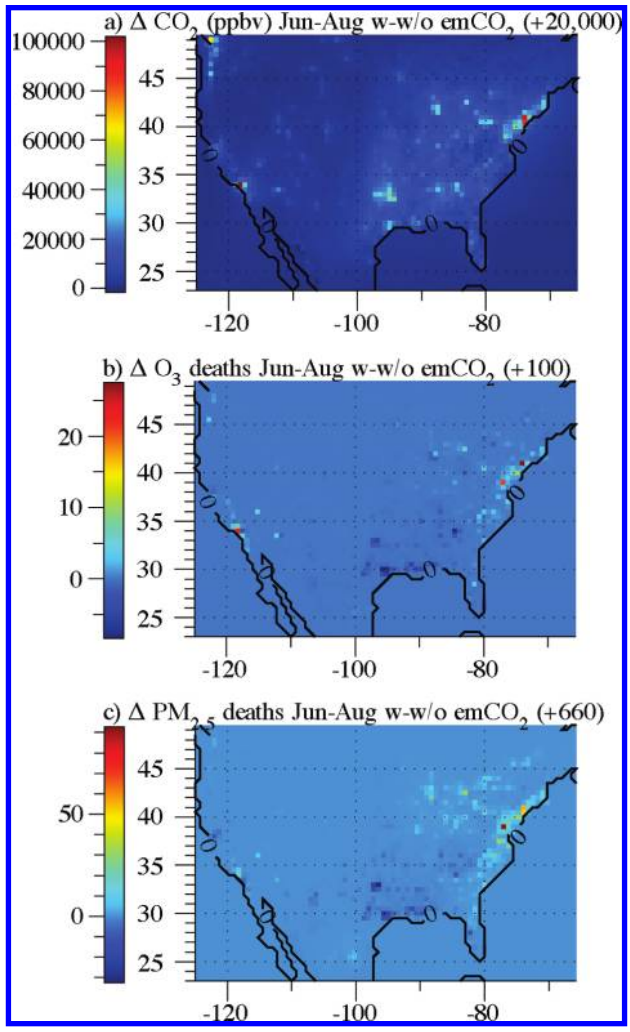

FIGURE 5. Same as Figure 2 but for the U.S. domain and for Jun-Aug. Numbers in parentheses Jun-Aug averaged changes (for CO_2) or total changes (for mortalities) over the domain.

areas. As such, CO_2 cap and trade, if done, should consider the location of emissions to avoid additional health damage.

Acknowledgments

Support came from the U.S. Environmental Protection Agency grant RD-83337101-O, NASA grant NX07AN25G, and the NASA High-End Computing Program.

Supporting Information Available

Model and emissions used for this study (Section 1), feedbacks in the model (Section 2), and a description of simulations (Section 3). This material is available free of charge via the Internet at http://pubs.acs.org.

Literature Cited

(1) Idso, C. D.; Idso, S. B.; Balling, R. C., Jr. The urban CO_2 dome of Phoenix, Arizona. *Phys. Geogr.* **1998**, *19*, 95–108.
(2) Idso, C. D.; Idso, S. B.; Balling, R. C., Jr. An intensive two-week study of an urban CO2 dome in Phoenix, Arizona, USA. *Atmos. Environ.* **2001**, *35*, 995–1000.
(3) Balling, R. C., Jr.; Cerveny, R. S.; Idso, C. D. Does the urban CO_2 dome of Phoenix, Arizona contribute to its heat island. *Geophys. Res. Lett.* **2001**, *28*, 4599–4601.
(4) Gratani, L.; Varone, L. Daily and seasonal variation of CO_2 in the city of Rome in relationship with the traffic volume. *Atmos. Environ.* **2005**, *39*, 2619–2624.
(5) Newman, S.; Xu, X.; Affek, H. P.; Stolper, E.; Epstein, S. Changes in mixing ratio and isotopic composition of CO_2 in urban air from the Los Angeles basin, California, between 1972 and 2003. *J. Geophys. Res.* **2008**, *113*, D23304, doi:10.1029/2008JD009999.
(6) Rigby, M.; Toumi, R.; Fisher, R.; Lowry, D.; Nisbet, E. G. First continuous measurements of CO_2 mixing ratio in central London using a compact diffusion probe. *Atmos. Environ.* **2008**, *42*, 8943–8953.
(7) Knowlton, K.; Rosenthal, J. E.; Hogrefe, C.; Lynn, B.; Gaffin, S.; Goldberg, R.; Rosenzweig, C.; Civerolo, K.; Ku, J.-Y.; Kinney, P. L. Assessing ozone-related health impacts under a changing climate. *Environ. Health Perspect.* **2004**, *112*, 1557–1563.
(8) Mickley, L. J.; Jacob, D. J.; Field, B. D.; Rind, D. Effects of future climate change on regional air pollution episodes in the United States. *Geophys. Res. Lett.* **2004**, *31*, L24103, doi:10.1029/2004GL021216.
(9) Steiner, A. L.; Tonse, S.; Cohen, R. C.; Goldstein, A. H.; Harley, R. A. Influence of future climate and emissions on regional air quality in California. *J. Geophys. Res.* **2006**, *111*, D18303, doi:10.1029/2005JD006935.
(10) Unger, N.; Shindell, D. T.; Koch, D. M.; Ammann, M.; Cofala, J.; Streets, D. G. Influences of man-made emissions and climate changes on tropospheric ozone, methane, and sulfate at 2030 from a broad range of possible futures. *J. Geophys. Res.* **2006**, *111*, D12313, doi:10.1029/2005JD006518.
(11) Liao, H.; Chen, W.-T.; Seinfeld, J. H. Role of climate change in global predictions of future tropospheric ozone and aerosols. *J. Geophys. Res.* **2006**, *111*, D12304, doi:10.1029/2005JD006852.
(12) Bell, M. L.; Goldberg, R.; Hogrefe, C.; Kinney, P. L.; Knowlton, K.; Lynn, B.; Rosenthal, J.; Rosenzweig, C.; Patz, J. A. Climate change, ambient ozone, and health in 50 U.S. cities. *Clim. Change* **2007**, *82*, 61–76.
(13) Jacobson, M. Z. On the causal link between carbon dioxide and air pollution mortality. *Geophys. Res. Lett.* **2008**, *35*, L03809, doi:10.1029/2007GL031101.
(14) Jacobson, M. Z.; Streets, D. G. The influence of future anthropogenic emissions on climate, natural emissions, and air quality. *J. Geophys. Res.* **2009**, *114*, D08118, doi:10.1029/2008JD011476.
(15) Jacobson, M. Z. GATOR-GCMM: 2. A study of day- and nighttime ozone layers aloft, ozone in national parks, and weather during the SARMAP Field Campaign. *J. Geophys. Res.* **2001**, *106*, 5403–5420.
(16) Jacobson, M. Z.; Kaufmann, Y. J.; Rudich, Y. Examining feedbacks of aerosols to urban climate with a model that treats 3-D clouds with aerosol inclusions. *J. Geophys. Res.* **2007**, *112*, doi:10.1029/2007JD008922.
(17) Jacobson, M. Z. The short-term effects of agriculture on air pollution and climate in California. *J. Geophys. Res.* **2008**, *113*, D23101, doi:10.1029/2008JD010689.
(18) Global Forecast System. 1°x1° reanalysis fields; 2007; http://nomads.ncdc.noaa.gov/data/ (accession July 1, 2008).
(19) *Estimating mortality risk reduction and economic benefits from controlling ozone air pollution*; National Research Council, The National Academies Press: Washington, DC, 2008.
(20) *Integrated science assessment for particulate matter, Second External Review Draft*; U.S. Environmental Protection Agency: 2008; EPA/600/R-08/139B.
(21) Johnson, S. L. California State Motor Vehicle Pollution Control Standards; Notice of Decision Denying a Waiver of Clean Air Act Preemption for California's 2009 and Subsequent Model Year Greenhouse Gas Emission Standards for New Motor Vehicles. *Fed. Register* **2008**, *73* (45), 12,156–12,169.
(22) *AIR Data*; United States Environmental Protection Agency: 2006; http://www.epa.gov/air/data/ (accession August 1, 2009).
(23) Thurston, G. D.; Ito, K. Epidemiological studies of acute ozone exposures and mortality. *J. Exposure Anal. Environ. Epidemiol.* **2001**, *11*, 286–294.
(24) Hoyert, D. L.; Heron, M. P.; Murphy, S. L.; Kung H.-C. National Vital Statistics Reports; Vol. 54, No. 13, 2006. http://www.cdc.gov/nchs/fastats/deaths.htm (accession August 1, 2009).
(25) Merrill, C. T.; Elixhauser, A. HCUP Fact Book No. 6: Hospitalization in the United States, 2002; Appendix, 2005. www.ahrq.gov/data/hcup/factbk6/factbk6e.htm (accession August 1, 2009).
(26) Mannino, D. M.; Homa, D. M.; Akinbami, L. J.; Moorman, J. E.; Gwynn, C.; Redd, S. C. Center for Disease Control Morbidity and Mortality Weekly Report. *Surveill. Summ.* **2002**, *51* (SS01), 1–13.
(27) Ostro, B. D.; Tran, H.; Levy, J. I. The health benefits of reduced tropospheric ozone in California. *J. Air Waste Manage. Assoc.* **2006**, *56*, 1007–1021.
(28) Pope III, C. A.; Burnett, R. T.; Thun, M. J.; Calle, E. E.; Krewski, D.; Ito, K.; Thurston, G. D. Lung cancer, cardiopulmonary mortality, and long-term exposure to fine particulate air pollution. *JAMA* **2002**, *287*, 1132–1141.
(29) Pope III, C. A.; Burnett, R. T.; Thurston, G. D.; Thun, M. J.; Calle, E. E.; Drewski, D.; Godleski, J. J. Cardiovascular mortality and long-term exposure to particulate air pollution. *Circulation* **2004**, *109*, 71–77.

ES903018M